

# Journal of Materials Chemistry A

Accepted Manuscript



This is an *Accepted Manuscript*, which has been through the Royal Society of Chemistry peer review process and has been accepted for publication.

*Accepted Manuscripts* are published online shortly after acceptance, before technical editing, formatting and proof reading. Using this free service, authors can make their results available to the community, in citable form, before we publish the edited article. We will replace this *Accepted Manuscript* with the edited and formatted *Advance Article* as soon as it is available.

You can find more information about *Accepted Manuscripts* in the [Information for Authors](#).

Please note that technical editing may introduce minor changes to the text and/or graphics, which may alter content. The journal's standard [Terms & Conditions](#) and the [Ethical guidelines](#) still apply. In no event shall the Royal Society of Chemistry be held responsible for any errors or omissions in this *Accepted Manuscript* or any consequences arising from the use of any information it contains.

## COMMUNICATION

# Synergistic Enhancement of Nitrogen and Sulfur Co-doped Graphene with Carbon Nanospheres Insertion for Electrocatalytic Oxygen Reduction Reaction

Cite this: DOI: 10.1039/x0xx00000x

Received 00th January 2012,

Accepted 00th January 2012

DOI: 10.1039/x0xx00000x

www.rsc.org/

Min Wu<sup>a</sup>, Jie Wang<sup>a</sup>, Zexing Wu<sup>a</sup>, Huolin L. Xin<sup>b</sup>, and Deli Wang<sup>a,\*</sup>

Carbon black incorporated nitrogen and sulfur co-doped graphene (NSGCB) nanocomposite has been synthesized through a one-pot annealing of a precursor mixture containing graphene oxide, thiourea, and acidized carbon black (CB). The NSGCB shows excellent performance for the oxygen reduction reaction (ORR) with the onset and half-wave potentials at 0.96 V and 0.81 V (vs. RHE), respectively. It is significantly improved over that of the catalysts derived from only graphene (0.90 V and 0.76V) or carbon nanosphere (0.82 V and 0.74V). The enhanced catalytic activity on the NSGCB electrode could be attributed to the synergistic effect of N/S co-doping and the enlarged interlayer space resulted from the insertion of carbon nanosphere into the graphene sheets. The four-electron selectivity and the limiting current density of the NSGCB nanocomposite are comparable to that of the commercially Pt/C catalyst. Furthermore, the NSGCB nanocomposite is superior to Pt/C in terms of long-term durability and tolerance to methanol poisoning.

## Introduction

The cathodic oxygen reduction reaction (ORR) plays a crucial role in various renewable energy applications such as fuel cells and metal-air batteries<sup>1, 2</sup>. Currently, platinum-based nanomaterials are considered as the most effective catalysts towards ORR<sup>3-5</sup>. However, the high-cost and poor stability of platinum, as well as low tolerance to methanol poisoning, have limited the commercialization of fuel cells. Therefore, it is vital important to develop durable and low-cost catalysts to replace platinum. Considerable efforts have been focused on non-noble metal and metal-free electrocatalysts<sup>6, 7</sup>. Among various metal-free catalysts, nitrogen doped (N-doped) carbons have been extensively studied. The electrocatalytic activity for ORR originates from the heteroatoms doping, making the catalysts non-electron-neutral and consequently facilitating oxygen adsorption and reduction<sup>1, 8, 9</sup>.

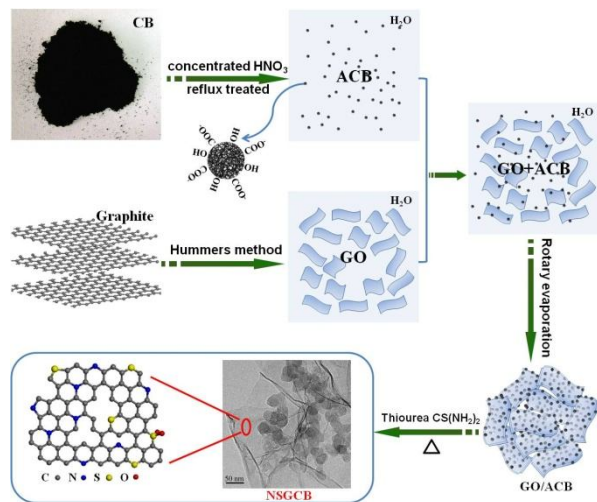
Recently, apart from N, other elements—B<sup>10</sup>, S<sup>11</sup>, P<sup>12, 13</sup>, and I<sup>14</sup>—have also been doped into carbon materials acting as high-performance metal-free catalysts for the ORR. More recently,

heteroatoms co-doped carbon materials have been investigated and exhibited enhanced ORR performance by creating synergistic non-electron-neutral sites. For instance, B/N co-doped carbon nanotubes<sup>15</sup> and graphene<sup>9, 16</sup> have shown better ORR performance compared with solely B or N doped materials. Even though various heteroatoms co-doped carbon materials<sup>8, 17-23</sup> have been developed as metal-free catalysts for the ORR, important kinetic parameters such as the onset potential and the limiting current density still need to be further improved. Herein, we report the synthesis of nitrogen and sulfur co-doped graphene/carbon black composite (NSGCB) as a metal-free electrocatalyst by annealing graphene oxide (GO), acidized carbon black (ACB), and thiourea in N<sub>2</sub> atmosphere at high temperature. Our electrochemical results display the as-synthesized nanocomposites exhibit an excellent ORR performance with superior durability and high tolerance to methanol poisoning compared with commercial Pt/C catalysts. Besides, it is noted that our NSGCB exhibited to be one of the best performance metal-free electrocatalysts for ORR in alkaline media (Table S1). Thiourea (CS(NH<sub>2</sub>)<sub>2</sub>), a low cost, low toxicity, solid compound, was used in this research as a sole heteroatom precursor for nitrogen and sulfur source, making the preparation more safe and cost effective. Besides, Vulcan XC-72R, one commercially carbon nanosphere commonly used as the support for platinum catalysts, was inserted into the graphene sheets to lessen the agglomeration of graphene sheets and consequently increase the interlayer space for efficient transport of the reactants, ions and electrons<sup>24, 25</sup>.

## Results and Discussion

The NSGCB nanocomposite was synthesized through a one-step doping procedure as illustrated in **Scheme 1**. The GO was first prepared by a modified Hummer's method<sup>26</sup> and dispersed in water for use. The ACB was achieved by refluxing carbon black in concentrated HNO<sub>3</sub> to remove the metal impurities and enhanced its wet ability. The mixture solution of GO and ACB (GO/ACB weight ratio of 3:1) was sonicated to form a homogenous aqueous solution. After removing of water by rotary evaporation, a black GO/ACB mixture powder was formed. The GO/ACB composite was then

annealed under a  $N_2$  atmosphere in the presence of thiourea (weight ratio of 1:10) at 900 °C to obtain NSGCB (see the Supporting Information for experimental details). Nitrogen and sulfur co-doped graphene sheets (NSGs), nitrogen and sulfur co-doped carbon black (NSCB), pristine graphene sheets (Gs) as well as pristine carbon black (CB) were also prepared under similar conditions for comparison.



**Scheme 1.** Schematic illustration of the preparation for NSGCB nanocomposite.

Fig. 1a shows the scanning TEM (STEM) images of the NSGCB. The typical nanocomposite contains graphene and carbon blacks, and the carbon blacks have a uniform diameter of 30 nm. The carbon nanospheres were inserted into the graphene sheets as expected (see also the Supporting Information, Fig. S1a and b). Energy dispersive spectroscopy (EDS) analysis of the selected area in Figure 1a clearly shows the existence of C, N and S in the nanocomposite. The doping of N and S into the NSGCB can be further disclosed by the elemental mapping images of carbon, nitrogen, and sulfur as shown in Figure 1d, e and f. A homogeneous distribution of S, N and C elements can be recognized in NSGCB. The results indicate that S and N were successfully doped into the NSGCB, which was also confirmed by the composite elemental maps of S, N and C (Supporting Information, Figure S1c). Considering that thiourea was completely decomposed at temperatures above 600 °C in  $N_2$ , as shown by thermal gravimetric analysis (TGA) (Supporting Information, Fig. S2), it is sound to believe the N and S atoms were truly doped into the NSGCB framework, rather than any residual precursor or byproduct.

The elemental information in the NSGCB composite was further revealed by X-ray photoelectron spectroscopy (XPS). The existence of C, O, N, and S can be clearly seen in the survey scan (Fig. 2a). The atomic percentage of N and S was calculated to be 4.9% and 1.1%, respectively. The asymmetrical C 1s spectra (Figure 2b) can be fitted into five peaks corresponding to C-C (284.5 eV), C-OH (285 eV), C=O (285.7 eV), C-S (283.9 eV) and C-N (287.2 eV)<sup>8, 27</sup>, further indicating that N and S have been doped into the carbon framework. The high resolution of N 1s spectrum (Figure 2c) reveals three species of N in NSGCB including Pyridinic N (398.1 eV), Pyrrolic N (399.2 eV), Graphitic N (401.2 eV), as typically observed in N-doped carbons<sup>28-30</sup>. Remarkably, the Graphitic N occupies the most content (55.6%) in the three type of N, which is known as the most activity type of N for ORR<sup>18, 24</sup>. Similarly, a detailed scan of S 2p (Figure 2d) mainly displays three different peaks. The two major

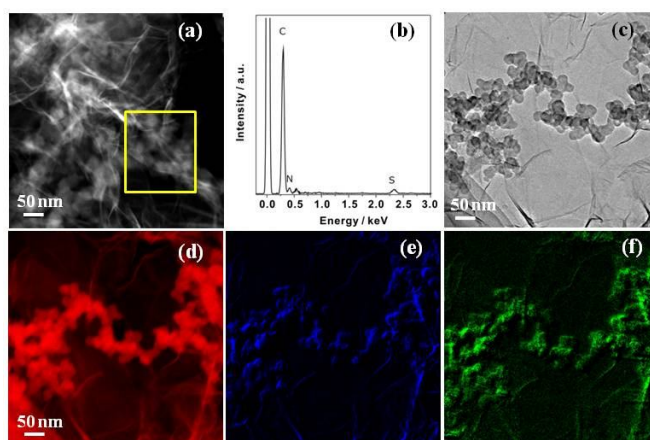


**Fig. 1** (a) STEM image of the typical NSGCB nanocomposite. (b) EDS analysis of the selected area in figure 1a. (c) TEM image of NSGCB nanocomposite and elemental mapping images of carbon (d), nitrogen (e), and sulfur (f) in the corresponding NSGCB.

peaks are consistent with the reported  $S_{2p_{3/2}}$  and  $S_{2p_{1/2}}$  which are attributed to the binding sulfur in -C-S- bonds and conjugated -C=S- bonds, respectively<sup>31</sup>. The third minor peaks at the binding energy of 168.6 eV belong to oxidized S (-SO<sub>x</sub>-), which are anticipated to occur at the edge of carbon skeleton<sup>19</sup>. According to the high-resolution XPS data, N and S also doped into the NSGs and NSCB, and their atom content (5.1 at.% and 1.4 at.%) in NSGs while (1.1 at.% and 0.5 at.%) in NSCB can be reached, respectively (see Supporting Information, Figure S3). These results indicated that thiourea could be used as precursor to prepare the nitrogen and sulfur dual-doped carbons<sup>22</sup>.

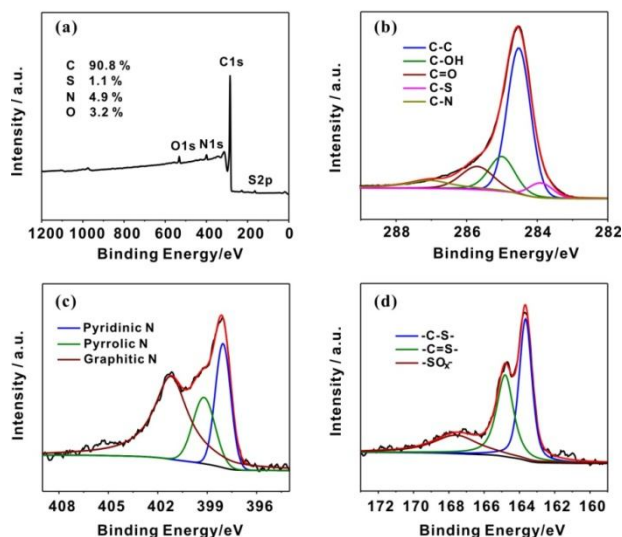


**Fig. 2** (a) XPS spectrum of the NSGCB nanocomposite, and the corresponding high-resolution spectrum of C 1s (b), N 1s (c), and S 2p (d).

Further structural information about the carbons was obtained from Raman spectroscopy (Fig. 3a) measurement. The typical D band deriving from the edges, defects and disordered carbon sites and the G band corresponding to  $E_{2g}$  vibration mode for  $sp^2$ -hybridized graphitic carbon were located around 1350  $cm^{-1}$  and 1580  $cm^{-1}$ , respectively<sup>9</sup>. The higher peak appeared at 2700  $cm^{-1}$  and 2910  $cm^{-1}$  can be ascribed to a combination of D+D and

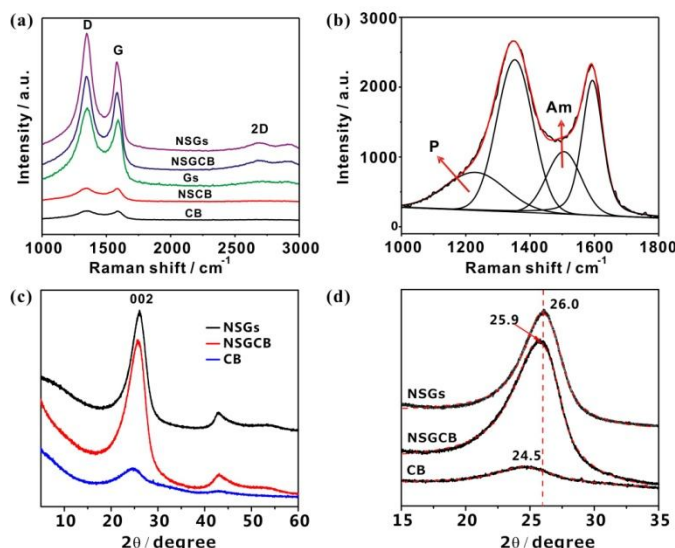


Fig. 3 (a) Raman spectra of different samples: as-received CB, Gs, NSCB, NSGs, and NSGCB. (b) Deconvolution of the Raman spectrum of NSGCB nanocomposite. (c) XRD patterns of CB, NSGs, and NSGCB. (d) Enlarged (002) diffraction peaks in Fig. 3c.

D+G bands. In the Raman spectra of carbons, the intensity ratio of D band and G band ( $I_D/I_G$ ) is an important index of the defects level. It can be seen from Figure 3a that the NSGs show higher  $I_D/I_G$  ratios (1.33) than Gs (1.14), attributing to the incorporation of defects caused by N- and S-doping, which increased D band by broking hexagonal symmetry of graphene<sup>10</sup>. The Raman bands of carbon black (e.g. CB, NSCB) are broader than those of graphene (Gs, and NSGs) as a result of the more presence of amorphous carbon<sup>32</sup>. Take NSGCB as an example, two additional peaks, hidden by the D and G bands, should be introduced to gain appropriate fittings, which have been attributed to amorphous carbon (Am peak at  $1500\text{ cm}^{-1}$ ) and polyene-like structure carbon (P peak at  $1220\text{ cm}^{-1}$ )<sup>32, 33</sup>. The XRD patterns in Fig. 3c and d clear show that the diffraction peaks of NSGCB shift toward lower angle, indicating that the expansion of interlayer spaces by inserting of carbon black in the graphene sheet. The nitrogen isothermal adsorption/desorption technique was used to investigate the porous features of the NSGCB, NSGs, and NSCB. According to Figure S4, the nitrogen-adsorption isotherm of NSGCB is a typical IV type with a distinct hysteresis loop in the medium- and high-pressure regions ( $P/P_0=0.5-1$ ), and the Brunauer–Emmett–Teller (BET) specific surface area for NSGCB was calculated to be  $496\text{ m}^2/\text{g}$ , which was much higher than that of NSGs ( $303\text{ m}^2/\text{g}$ ) and NSCB ( $238\text{ m}^2/\text{g}$ ). This suggests that the carbon nanospheres were inserted into the graphene sheets and increased the interlayer space. Notably, upon the insertion of carbon nanospheres to graphene sheets, the average pore volume significantly increased from  $0.71\text{ cm}^3/\text{g}$  for NSGs to  $1.76\text{ cm}^3/\text{g}$  for NSGCB. These increased interlayer space and pore volumes are expected to facilitate the diffusion of reactants in the ORR process<sup>33</sup>.

The ORR catalytic performance of NSGCB was first measured by cyclic voltammetry (CV). As shown in Fig. 4a, a significant enhancement of the oxygen reduction peak at  $0.78\text{ V}$  (vs. RHE) in  $\text{O}_2$ -saturated electrolyte compared to featureless voltammetric current in  $\text{N}_2$ -saturated  $0.1\text{ M KOH}$  solution, indicating an excellent electrocatalytic activity of the NSGCB towards ORR. To further investigate the ORR kinetics on NSGCB, linear sweep voltammetry (LSV) polarization curves on a rotating disk electrode (RDE) were recorded at rotation rates range from  $400$  to  $2000\text{ rpm}$  and a scan rate of  $5\text{ mV s}^{-1}$  in  $\text{O}_2$ -saturated  $0.1\text{ M KOH}$  electrolyte. NSGCB exhibited a well-defined platform of diffusion-limiting currents

below  $0.65\text{ V}$  at all rotational speeds, indicating a high-performance electrocatalytic activity for ORR with a direct four-electron transfer pathway. And they also revealed a good linear relationship (see the insert in Fig. 4b) when converted them according to Koutecky–Levich plots ( $J^{-1}$  versus  $\omega^{-1/2}$ ) at  $0.6, 0.65, 0.7$  and  $0.75\text{ V}$  (analogous curves for the NSGs and NSCB are given in Figure S5). To investigate the effect of heteroatoms co-doping and carbon black on ORR catalytic activity, LSV curves of different electrocatalysts (Fig. 4c) for ORR were obtained on RDE in an  $\text{O}_2$ -saturated  $0.1\text{ M KOH}$  electrolyte. The NSGCB exhibits an onset and half-wave potentials at  $0.96\text{ V}$  and  $0.81\text{ V}$  (vs. RHE), respectively, which are much higher than those of NSGs ( $0.90\text{ V}$  and  $0.76\text{ V}$ ) and NSCB ( $0.82\text{ V}$  and  $0.74\text{ V}$ ). Moreover, NSGCB also showed much higher limiting diffusion current density compared to NSCB and NSGs, the enhanced catalytic activity on NSGCB electrode could be resulted from the enlarged interlayer space which is beneficial to mass transfer. Meanwhile, it can be clearly seen that the ORR catalytic activity of NSGCB is almost equal to that of commercial Pt/C ( $20\text{ wt}\%$ ) in alkaline condition. For a better understanding of the ORR catalytic activities of the synthesized electrocatalysts, the Tafel-plots and mass activities at  $0.70$  and  $0.80\text{ V}$  for NSGCB, NSGs, and NSCB were compared in Figure S6 and Figure 4d. It can be seen clearly that NSGCB exhibited much higher mass activity and onset potential than both NSCB and NSGs.

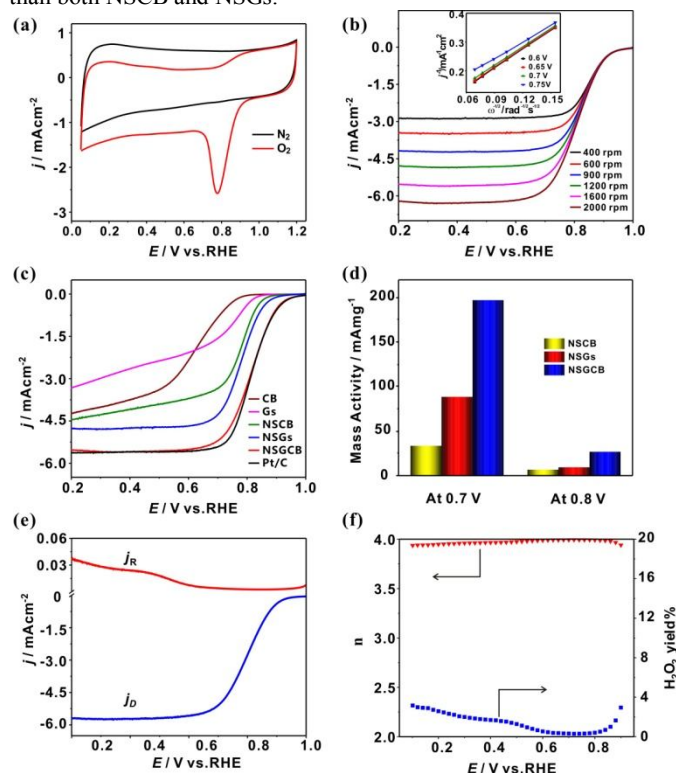


Fig. 4 (a) CV curves of NSGCB in  $\text{O}_2$ - and  $\text{N}_2$ -saturated  $0.1\text{ M KOH}$  electrolyte at a scan rate of  $50\text{ mVs}^{-1}$ ; (b) LSVs of NSGCB at different rotating speeds; the inset shows the Koutecky–Levich plots for NSGCB at different potentials; (c) ORR polarization curves on different electrodes at a rotation rate of  $1600\text{ rpm}$  and scan rate of  $5\text{ mVs}^{-1}$ ; (d) Comparison of mass activities for NSCB, NSGs and NSGCB at  $0.7$  and  $0.8\text{ V}$ ; (e) RRDE voltammograms of NSGCB at a rotating speed of  $1600\text{ rpm}$ ; (f) The electron-transfer number  $n$  and  $\text{H}_2\text{O}_2$  yield for NSGCB catalyst.

To further investigate the kinetics of ORR on NSGCB, rotating ring disk electrode (RRDE) voltammograms was performed at the

rotation rate of 1600 rpm in O<sub>2</sub>-saturated 0.1 M KOH solution with a scanning rate of 5 mV s<sup>-1</sup>. As shown in Fig. 4e, the disk show a high limiting current density at approximately 5.68 mA cm<sup>-2</sup>, which is in accordance with the RDE characterization. The electron transfer number (n) and hydrogen peroxide production were calculated via the following equations (1-2):

$$n = \frac{4j_D}{j_D + \frac{j_R}{N}} \quad (1)$$

$$H_2O_2 \% = \frac{\frac{2j_R}{N}}{j_D + \frac{j_R}{N}} \times 100\% \quad (2)$$

$j_D$  is the faradaic disk current,  $j_R$  is the faradaic ring current, and N is the collection efficiency (0.37) of the ring electrode. Remarkably, the n of 3.93 to 3.99 was achieved in the voltage range of 0.1 and 0.9 V, while the H<sub>2</sub>O<sub>2</sub> yielding is less than 4 % in this long voltage range. Apparently, the ORR catalyzed by NSGCB is almost exactly through the four electron (4e) transfer pathway and comparable to that of commercial Pt/C (Supporting Information, Fig. S7).

Given that the potential of NSGCB as efficient metal-free ORR catalysts to substitute the commercially Pt/C electrode, we further measured the electrochemical stability, and tolerance for methanol crossover, which are two major considerations for practical application in fuel cells. The durability of the catalysts was studied using current-time (i-t) chronoamperometric method, which was performed at a constant potential of 0.7 V (vs. RHE) for 15,000 seconds in O<sub>2</sub>-saturated 0.1 M KOH solution with a rotating speed of 1600 rpm (Fig. 5a). Noteworthy, i-t curve of NSGCB exhibits negligible current decay (~5%). In contrast, the current on Pt/C gradually decreased, with a current loss up to 27% after 15,000 seconds. The methanol tolerance performance was measured by introducing 3 M methanol into the O<sub>2</sub>-saturated 0.1 M KOH solution. As shown in Fig. 5b, the Pt/C electrode shows a sharp decrease in current at 200 s, while the amperometric current on the NSGCB electrode exhibits a negligible decay with the addition of methanol. These results clearly indicate that the catalytic active sites on the NSGCB are much more stable than those on the commercial Pt/C electrode and have high potential application in methanol based and alkaline fuel cells.

## Conclusion

In the present research, we have developed N- and S- co-doped graphene/carbon black composite as metal-free electrocatalyst by pyrolysis of GO, acidized carbon black, and thiourea under N<sub>2</sub> atmosphere at 900 °C. The high specific area resulted from intercalation of carbon nanospheres between graphene sheets and dual-doping of N, S afford abundant catalytic sites on the surface of the NSGCB and facilitate the electrolyte/reactant diffusion during the oxygen reduction process. Due to a synergetic effect arising from dual-doping and high specific area, the resultant NSGCB electrode has enhanced electrocatalytic activity for ORR in alkaline medium compared with its counterparts (i.e., NSGs or NSCB). Besides, the observed superior ORR performance of NSGCB was comparable to that of commercial Pt/C materials but with higher durability and excellent tolerance to methanol. Moreover, the synthetic strategy toward NSGCB is very simple and suitable for mass production, and the as-obtained N/S co-doping carbon composite has potential applications in fuel cells, and other metal-air batteries.

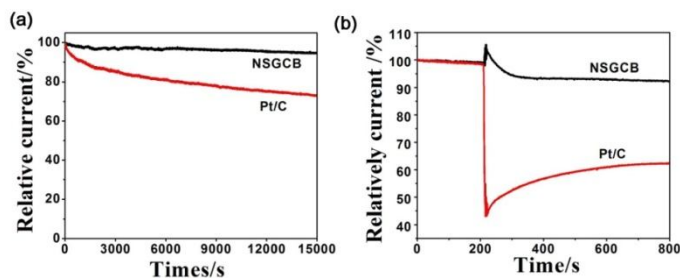


Fig. 5 (a) Durability evaluation of NSGCB nanocomposite and Pt/C at 0.7 V (vs. RHE) for 15000 s with a rotation rate of 1600 rpm. (b) i-t chronoamperometric response of NSGCB and Pt/C in 0.1 M KOH solution with introduction of 3 M methanol after about 200 s.

## Acknowledgements

This work was supported by the National Science Foundation of China(21306060), the Program for New Century Excellent Talents in Universities of China (NCET-13-0237), the Doctoral Fund of Ministry of Education of China (20130142120039), the Fundamental Research Funds for the Central University (2013TS136, 2014YQ009). This research carried out in part at the Center for Functional Nanomaterials, Brookhaven National Laboratory, which is supported by the U.S. Department of Energy, Office of Basic Energy Sciences, under Contract No.DE-SC0012704. We thank Analytical and Testing Center of Huazhong University of Science & Technology for allowing us to use its facilities.

## Notes and references

<sup>a</sup> Key Laboratory for Large-Format Battery Materials and System, Ministry of Education, School of Chemistry and Chemical Engineering, Huazhong University of Science & Technology, Wuhan, 430074, P.R. China. E-mail: wangdl81125@hust.edu.cn.

<sup>b</sup> Center for Functional Nanomaterials, Brookhaven National Laboratory, Upton, NY, USA; Department of Materials Science and Engineering SUNY Stony Brook University, Stony Brook, NY, 11794, USA

Electronic Supplementary Information (ESI) available: [details of experimental procedures, additional TEM, XPS spectra, TGA curves and electrochemical performance]. See DOI: 10.1039/c000000x/

1. K. P. Gong, F. Du, Z. H. Xia, M. Durstock and L. M. Dai, *Science*, 2009, **323**, 760.
2. Y. Xiang, S. F. Lu and S. P. Jiang, *Chem. Soc. Rev.*, 2012, **41**, 7291.
3. N. Cheng, M. N. Banis, J. Liu, A. Riese, X. Li, R. Li, S. Ye, S. Knights and X. Sun, *Adv. Mater.*, 2015, **27**, 277.
4. D. L. Wang, H. L. L. Xin, R. Hovden, H. S. Wang, Y. C. Yu, D. A. Muller, F. J. DiSalvo and H. D. Abruna, *Nat. Mater.*, 2013, **12**, 81.
5. N. Cheng, M. N. Banis, J. Liu, A. Riese, S. Mu, R. Li, S. T.-K. and X. Sun, *Energy & Environ. Sci.*, 2015, DOI: 10.1039/C4EE04086D.
6. C. Z. Zhang, R. Hao, H. B. Liao and Y. L. Hou, *Nano Energy*, 2013, **2**, 88.
7. H. Yin, C. Z. Zhang, F. Liu and Y. L. Hou, *Adv. Funct. Mater.*, 2014, **24**, 2930.

8. J. Liang, Y. Jiao, M. Jaroniec and S. Z. Qiao, *Angew. Chem. Int. Ed.*, 2012, **51**, 11496.
9. S. Y. Wang, L. P. Zhang, Z. H. Xia, A. Roy, D. W. Chang, J. B. Baek and L. M. Dai, *Angew. Chem. Int. Ed.*, 2012, **51**, 4209.
10. L. J. Yang, S. J. Jiang, Y. Zhao, L. Zhu, S. Chen, X. Z. Wang, Q. Wu, J. Ma, Y. W. Ma and Z. Hu, *Angew. Chem. Int. Ed.*, 2011, **50**, 7132.
11. Z. Yang, Z. Yao, G. F. Li, G. Y. Fang, H. G. Nie, Z. Liu, X. M. Zhou, X. Chen and S. M. Huang, *ACS Nano*, 2012, **6**, 205.
12. Z. W. Liu, F. Peng, H. J. Wang, H. Yu, W. X. Zheng and J. A. Yang, *Angew. Chem. Int. Ed.*, 2011, **50**, 3257.
13. D. S. Yang, D. Bhattacharjya, S. Inamdar, J. Park and J. S. Yu, *J. Am. Chem. Soc.*, 2012, **134**, 16127.
14. Z. Yao, H. G. Nie, Z. Yang, X. M. Zhou, Z. Liu and S. M. Huang, *Chem. Commun.*, 2012, **48**, 1027.
15. S. Y. Wang, E. Iyyamperumal, A. Roy, Y. H. Xue, D. S. Yu and L. M. Dai, *Angew. Chem. Int. Ed.*, 2011, **50**, 11756.
16. Y. Zheng, Y. Jiao, L. Ge, M. Jaroniec and S. Z. Qiao, *Angew. Chem. Int. Ed.*, 2013, **52**, 3110.
17. Y. Zhao, L. J. Yang, S. Chen, X. Z. Wang, Y. W. Ma, Q. Wu, Y. F. Jiang, W. J. Qian and Z. Hu, *J. Am. Chem. Soc.*, 2013, **135**, 1201.
18. X. Wang, J. Wang, D. L. Wang, S. O. Dou, Z. L. Ma, J. H. Wu, L. Tao, A. L. Shen, C. B. Ouyang, Q. H. Liu and S. Y. Wang, *Chem. Commun.*, 2014, **50**, 4839.
19. Y. Z. Su, Y. Zhang, X. D. Zhuang, S. Li, D. Q. Wu, F. Zhang and X. L. Feng, *Carbon*, 2013, **62**, 296.
20. Q. Q. Shi, F. Peng, S. X. Liao, H. J. Wang, H. Yu, Z. W. Liu, B. S. Zhang and D. S. Su, *J. Mater. Chem. A*, 2013, **1**, 14853.
21. J. X. Xu, G. F. Dong, C. H. Jin, M. H. Huang and L. H. Guan, *Chemsuschem*, 2013, **6**, 493.
22. Z. Liu, H. G. Nie, Z. Yang, J. Zhang, Z. P. Jin, Y. Q. Lu, Z. B. Xiao and S. M. Huang, *Nanoscale*, 2013, **5**, 3283.
23. W. Ai, Z. Luo, J. Jiang, J. Zhu, Z. Du, Z. Fan, L. Xie, H. Zhang, W. Huang and T. Yu, *Adv. Mater.*, 2014, **26**, 6186.
24. P. Chen, T. Y. Xiao, Y. H. Qian, S. S. Li and S. H. Yu, *Adv. Mater.*, 2013, **25**, 3192.
25. C. H. Choi, M. W. Chung, H. C. Kwon, J. H. Chung and S. I. Woo, *Appl. Catal. B-Environ.*, 2014, **144**, 760.
26. W. S. Hummers and R. E. Offeman, *J. Am. Chem. Soc.*, 1958, **80**, 1339.
27. Y. Q. Chang, F. Hong, C. X. He, Q. L. Zhang and J. H. Liu, *Adv. Mater.*, 2013, **25**, 4794.
28. Y. Wang, Y. Y. Shao, D. W. Matson, J. H. Li and Y. H. Lin, *ACS Nano*, 2010, **4**, 1790.
29. D. S. Geng, Y. Chen, Y. G. Chen, Y. L. Li, R. Y. Li, X. L. Sun, S. Y. Ye and S. Knights, *Energy & Environ. Sci.*, 2011, **4**, 760.
30. Z. Y. Lin, G. H. Waller, Y. Liu, M. L. Liu and C. P. Wong, *Nano Energy*, 2013, **2**, 241.
31. S. B. Yang, L. J. Zhi, K. Tang, X. L. Feng, J. Maier and K. Mullen, *Adv. Funct. Mater.*, 2012, **22**, 3634.
32. L. Bokobza, J. L. Bruneel and M. Couzi, *Chem. Phys. Lett.*, 2013, **590**, 153.
33. Q. Liu, H. Y. Zhang, H. W. Zhong, S. M. Zhang and S. L. Chen, *Electrochim. Acta*, 2012, **81**, 313.